The EMBO Journal (2004) 23, 1402–1410 | © 2004 European Molecular Biology Organization | All Rights Reserved 0261-4189/04
www.embojournal.org

THE EMBO JOURNAL

Erratum

Structural basis for recruitment of the ATPase activator Aha1 to the Hsp90 chaperone machinery

Philippe Meyer *et al*

The EMBO Journal (2004) **23,** 1402–1410. doi:10.1038/sj.emboj.7600141

Correction to: *The EMBO Journal* (2004) **23**, 511–519. doi:10.1038/sj.emboj.7600060

Due to an error, the colour images of some Figures within this paper were reproduced in mono. The correct colour versions of the figures, plus the full article are reproduced below:

Structural basis for recruitment of the ATPase activator Aha1 to the Hsp90 chaperone machinery

Philippe Meyer[1,4,5], Chrisostomos Prodromou[1,5], Chunyan Liao[2], Bin Hu[2], S Mark Roe[1], Cara K Vaughan[1], Ignacija Vlasic[2], Barry Panaretou[2], Peter W Piper[3,6] and Laurence H Pearl[1,*]

[1]Chester Beatty Laboratories, Section of Structural Biology, The Institute of Cancer Research, London, UK, [2]Division of Life Sciences, King's College London, London, UK and [3]Department of Biochemistry and Molecular Biology, University College London, London, UK

Hsp90 is a molecular chaperone essential for the activation and assembly of many key eukaryotic signalling and regulatory proteins. Hsp90 is assisted and regulated by co-chaperones that participate in an ordered series of dynamic multiprotein complexes, linked to Hsp90s conformationally coupled ATPase cycle. The co-chaperones Aha1 and Hch1 bind to Hsp90 and stimulate its ATPase activity. Biochemical analysis shows that this activity is dependent on the N-terminal domain of Aha1, which interacts with the central segment of Hsp90. The structural basis for this interaction is revealed by the crystal structure of the N-terminal domain (1–153) of Aha1 (equivalent to the whole of Hch1) in complex with the middle segment of Hsp90 (273–530). Structural analysis and mutagenesis show that binding of N-Aha1 promotes a conformational switch in the middle-segment catalytic loop (370–390) of Hsp90 that releases the catalytic Arg 380 and enables its interaction with ATP in the N-terminal nucleotide-binding domain of the chaperone.

The EMBO Journal (2004) **23,** 511–519. doi:10.1038/sj.emboj.7600060; Published online 22 January 2004
Subject Categories: proteins; structural biology
Keywords: co-chaperone; molecular chaperone; regulation

*Corresponding author. Chester Beatty Laboratories, Section of Structural Biology, The Institute of Cancer Research, 237 Fulham Road, London SW3 6JB, UK. Tel.: +44 0207 970 6045/6; Fax: +44 0207 970 6051; E-mail: laurence.pearl@icr.ac.uk
[4]Present address: Laboratoire d'Enzymologie et de Biochimie Structurales, CNRS, Avenue de la Terrasse, 91198 Gif sur Yvette, France
[5]These authors made equal contributions
[6]Present address: Department of Molecular Biology and Biotechnology, The University of Sheffield, Firth Court, Western Bank, Sheffield S10 2TN, UK

Received: 24 June 2003; accepted: 9 December 2003; published online: 22 January 2004

Introduction

The activation and/or stability of many of the key regulatory and signalling proteins of the eukaryotic cell depends on their interaction with the Hsp90 molecular chaperone. Hsp90s chaperone activity is itself absolutely dependent on binding and hydrolysis of ATP (Obermann *et al*, 1998; Panaretou *et al*, 1998), which drives a conformational cycle, involving opening and closing of a dimeric 'molecular clamp' via transient association of the N-terminal domains (Chadli *et al*, 2000; Prodromou *et al*, 2000). How this ATPase cycle in Hsp90 is coupled to activation and/or stabilisation of its client proteins is very poorly understood.

Hsp90 function is associated with a set of Hsp90-binding co-chaperones that variously assist client-protein recruitment or release, and modulate progress through the ATPase-coupled chaperone cycle (reviewed in Pearl and Prodromou, 2002). Hop/Sti1 is associated with the early phase of the cycle and helps recruit Hsp70-bound client proteins such as steroid hormone receptors to the Hsp90 system (Chen *et al*, 1996; Chen and Smith, 1998). Cdc37/p50^{cdc37} has a similar function, but is specific for the recruitment of protein kinases with which it interacts directly

(Grammatikakis *et al*, 1999). As well as their involvement in client-protein recruitment, both Hop/Sti1 and Cdc37/p50^{cdc37} have regulatory roles, and inhibit the ATPase cycle of Hsp90 (Prodromou *et al*, 1999; Siligardi *et al*, 2002). Sba1/p23 binds specifically to the ATP-bound state of Hsp90 in which the N-terminal domains are associated (Chadli *et al*, 2000; Prodromou *et al*, 2000), slowing down the ATPase cycle (Panaretou *et al*, 2002) and enhancing client-protein release (Young and Hartl, 2000). Recently, we identified a new co-chaperone, Aha1 (Panaretou *et al*, 2002), related to Hch1, a high-copy number suppressor of an Hsp90 temperature-sensitive allele (Nathan *et al*, 1999). In yeast, Aha1 and Hch1 were found to be required for Hsp90-dependent activation of an authentic client protein, and *in vitro* bound directly to Hsp90 stimulating its weak inherent ATPase activity by >12-fold. To gain some insight into the nature of the interaction between Hsp90 and Aha1/Hch1 and the mechanism by which Hsp90 ATPase is activated, we have now determined the crystal structure of a complex between the middle segment of Hsp90 (M-Hsp90) and the N-terminal domain of Aha1 (N-Aha1), equivalent to the entirety of Hch1. The structure reveals a novel fold for N-Aha1, and an extensive interface with Hsp90 involving all three subdomains of M-Hsp90. Binding of N-Aha1 elicits conformational changes in the catalytic loop of M-Hsp90, and suggests a mechanism for Hsp90 ATPase activation by the Aha1/Hch1 co-chaperone family.

Results

Defining the Hsp90–Aha1 core interaction

As attempts to co-crystallise full-length Aha1 with full-length Hsp90 have not been successful so far, we sought to identify interacting regions of the two proteins that would be more amenable to structural study. Previous structural and functional studies of the middle segment of Hsp90 had suggested that a significant component of the interaction with Aha1 was mediated by this part of the chaperone (Meyer *et al*, 2003), and this was analysed further by isothermal titration calorimetry (ITC). Although substantial binding was observed between full-length Aha1 and the Hsp90(273–560) fragment ($K_d = 3.8 \pm 1.4\,\mu M$), maximal affinity between the two proteins required full-length Hsp90 ($K_d = 0.67 \pm 0.07\,\mu M$), suggesting that some additional interactions with the N-terminal and/or C-terminal domains of Hsp90 were involved. However no significant interaction was observed between Aha1 and either of those domains in isolation, confirming that the middle segment of the chaperone provided the core of the interaction with Aha1. Similarly, while full-length Aha1 gave the maximal observed stimulation of Hsp90s ATPase activity, we had previously shown that a substantial degree of stimulation could be obtained with the smaller homologue Hch1 and with an N-terminal segment of Aha1 (residues 1–153) corresponding to the Hch1-homologous region (Panaretou *et al*, 2002), suggesting that this region provides the core of the interaction with Hsp90. Consistent with this, the N-terminal Aha1 segment (1–153) bound Hsp90 with significant affinity ($K_d = 1.75 \pm 0.15\,\mu M$). Taken together, these data identify M-Hsp90 and N-Aha1 as the main interacting parts of the proteins, which was confirmed by ITC measurement ($K_d = 3.3 \pm 0.8\,\mu M$).

On the basis of these results, crystallisation screens were conducted with approximately equimolar mixtures of Aha1(1–153) and an Hsp90 middle domain construct (273–530). Two crystal forms giving useful diffraction were obtained (see Materials and methods), and the structure of the better diffracting form was phased by molecular replacement with the previously determined structure of the isolated Hsp90 middle segment (Meyer *et al*, 2003). The structure of Aha1(1–153) was constructed from clear difference Fourier maps, and the complex was refined at 2.15 Å. The second crystal form diffracting to 2.7 Å contained four copies of the complex in the asymmetric unit and was solved by molecular replacement using the refined complex structure from the higher-resolution crystals.

Structure of the Aha1 N-terminal domain

Aha1(1–153) itself is an elongated cylindrical structure, ≈ 65 Å long with a diameter of ≈ 25 Å. The structure is formed by an N-terminal α-helix leading into a four-stranded meandering antiparallel β-sheet, followed by a C-terminal α-helix (Figure 1). The two helices are packed together on one side of the cylinder, with the β-sheet curving around them, so that its convex face forms the other side of the cylinder. The connecting loops between helix 1 and strand a, and between strands b and c, at the 'top' end of the cylinder are disordered in the smaller crystal form, but take up ordered conformations due to crystal packing interactions in two of the complexes in the larger crystal form. Comparison of the Aha1(1–153) structure with the CATH structural database (Pearl *et al*, 2000) identified only a single structure of related fold (PDB: 1BP1, CATH code 3.15.10.10). This is a domain from a human lipid-binding extracellular glycoprotein involved in antibacterial defences (Beamer *et al*, 1997), for which no other structural relatives have been identified and with no obvious evolutionary relationship to Aha1 either in function or cellular localisation.

Structure of the Hsp90–Aha1 core complex

Within the high-resolution crystal form, Aha1(1–153) interacts with two symmetry-related Hsp90(273–530) molecules on opposite sides of its cylindrical structure (Figure 2A). On one side, a small hydrophobic patch formed by the aromatic ring edges of Trp 19 and Tyr 23 of Aha1 packs against the exposed face of Trp 300 of Hsp90. This interaction does not occur in the larger crystal form, suggesting that it is a lattice contact. However, as Trp 300 is directly implicated in productive client-protein binding to Hsp90 (Meyer *et al*, 2003), this small hydrophobic 'patch' contact may be mimicking the kind of interactions Hsp90 makes with client proteins (Figure 2B).

The opposite side of the Aha1 molecule makes substantial and extensive interactions with Hsp90, along the entire length of both molecules and involving all three subdomains of the Hsp90 middle segment (Figure 3A). The Hsp90–Aha1 complex generated by this interaction is present in both crystal forms, suggesting that it is the biologically relevant unit. The core of the interaction with Aha1 is provided by the hydrophobic side chains of Leu 315, Ile 388 and Val 391 from the first domain of the Hsp90 middle segment, which pack against side chains of Ile 64, Leu 66 and Phe100 of Aha1 (Figure 3B). This hydrophobic interface is supported by polar

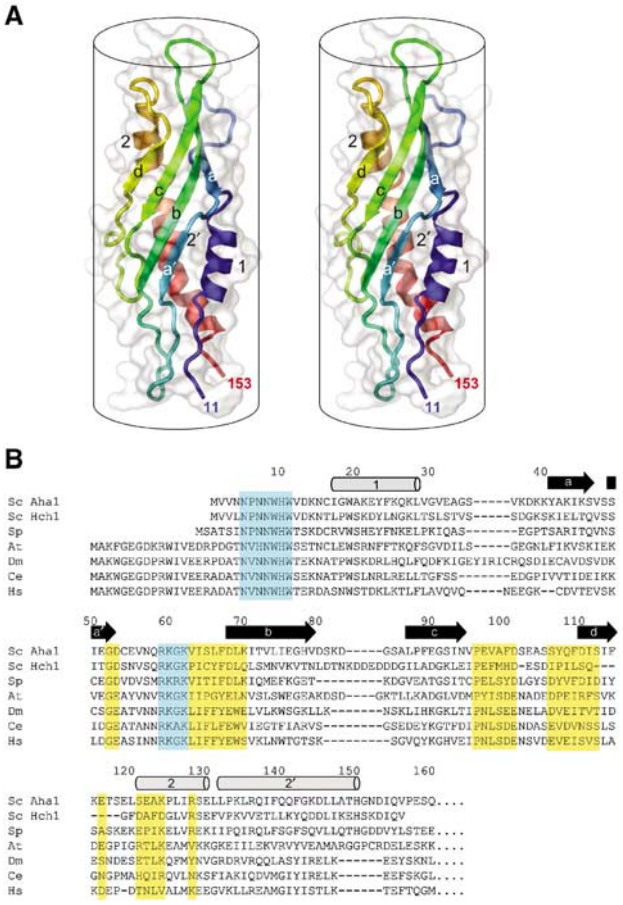

Figure 1 Aha1 N-terminal domain structure. (**A**) Secondary structure cartoon of the N-terminal domain of Aha1 (residues 1–153) rainbow coloured (blue→red) from the N- to C-terminus of the domain. The molecule has an overall cylindrical structure. (**B**) Alignment of the sequences for the N-terminal domains of representative Aha1 homologues from budding yeast (Sc), fission yeast (Sp), plants (At), flies (Dm), worms (Ce) and humans (Hs), and the entire sequence of the yeast Hch1 (Sc). Secondary structural elements are marked as in (A). The strongly conserved Trp/Asn-rich and basic motifs are highlighted in blue; regions involved in contacts with Hsp90 (see below) are highlighted in yellow.

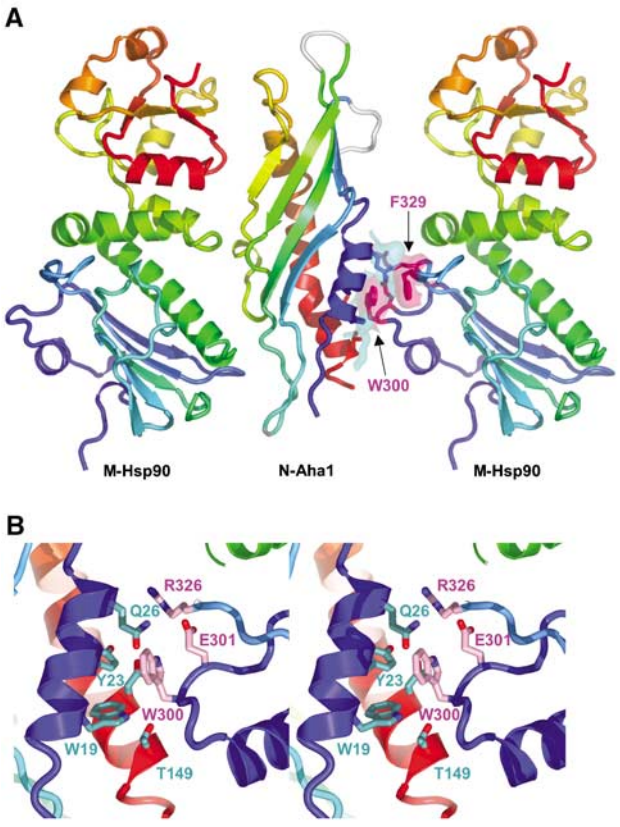

Figure 2 Hsp90–Aha1 lattice contacts imitating client-protein interactions. (**A**) Two consecutive Hsp90 middle-segment molecules in different asymmetric units in the high-resolution crystal form, both make contact with an Aha1 N-domain molecule. The highlighted interactions between the right-hand M-Hsp90 molecule and N-Aha1 are lattice contacts that do not occur in the second crystal form. However, these involve residues in Hsp90 that have been implicated in interactions with client proteins (Sato *et al*, 2000; Meyer *et al*, 2003), and suggest that this contact may reflect the kind of interaction Hsp90 makes with client proteins. (**B**) Detailed view of the interaction between the exposed hydrophobic side chain of Trp 300 in the putative client-binding site of Hsp90, and a shallow hydrophobic recess on the outer face of Aha1.

interactions between the side chain of Gln 314 from Hsp90 and the main chain of Ile 64-Ser 65 of Aha1. Higher up on the first domain of the middle segment of Hsp90, lysine residues 387, 390, 394 and 398 on the exposed face of the long amphipathic helix (387–409) form an extensive network of hydrogen bonding and ion-pair interactions with Asp 53, Asp 68, Glu 97 and Asp 101 from Aha1. The helical coil segment connecting the two αβα domains of the Hsp90 middle segment is involved in reciprocal side-chain to main-chain interactions involving Gln 434 of Hsp90 and Gln 108 of Aha1, reinforced by a hydrophobic interaction between the side chains of Thr 433 of Hsp90 and Pro 96 of Aha1. The small αβα domain of Hsp90 interacts via ion pairs involving Lys 469, Lys 514 and Glu 515 from Hsp90, and Glu 122, Asp 110 and Arg 128 of Aha1, respectively. Apart from the close-packed hydrophobic interaction between Aha1 and the first domain of the Hsp90 middle segment, the interface is relatively open and polar with an extensive network of solvent bridges between the two proteins, and a complementary pattern of charged patches on the opposing surfaces. The polar nature of much of this interface explains the previously observed sensitivity of the Aha1–Hsp90 interaction to high salt (Panaretou *et al*, 2002).

Although no crystal structures for a full-length Hsp90 molecule have yet been reported, it has been possible to construct a working model for the majority of the Hsp90 molecule from the structures of the separate N-terminal and middle segments (Prodromou *et al*, 1997; Meyer *et al*, 2003). By superimposing the Hsp90 component of the Aha1(1–153)–Hsp90(273–530) complex structure described here onto that reconstructed Hsp90 model, the orientation and interactions of Aha1 with respect to the full Hsp90 structure can be defined. In this complex, the visible N- and C-termini of the Aha1(1–153) are both directed towards the N-terminal nucleotide-binding domain of Hsp90 (Figure 4A). The C-terminus of this N-terminal Aha1 construct corresponds approximately to the true C-terminus of the smaller Hch1 homologues, found only in some simple yeasts. However, in the longer Aha1 proteins, the visible C-terminus would lead into an ~200 residue C-terminal domain whose structure is as yet unknown.

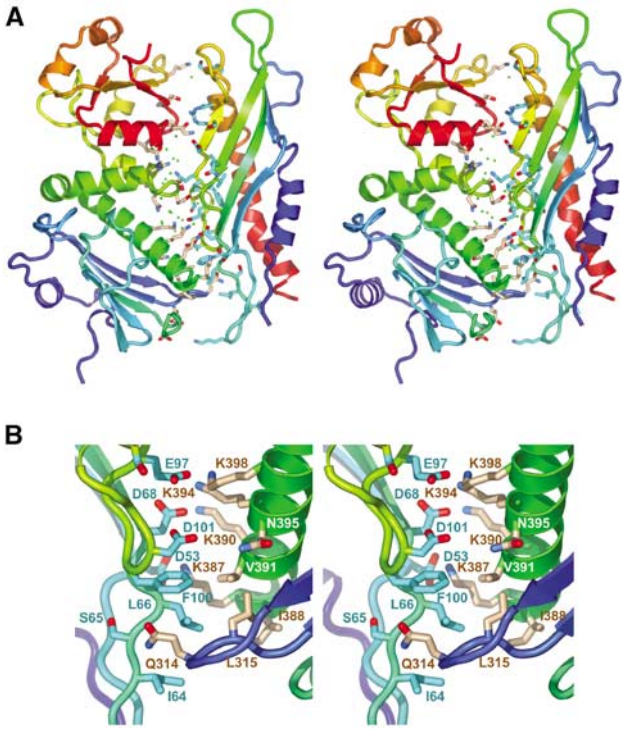

Figure 3 Hsp90–Aha1 complex. (**A**) The middle segment of Hsp90 contacts the Aha1 N-terminal domain over the entire length of both molecules, with interactions involving all three subdomains of M-Hsp90. Apart from a core hydrophobic interaction (see (B)), the interface involves many ion pairs and direct and solvent bridged polar interactions. Solvent molecules bound at the interface are show as green spheres. (**B**) Detailed view of the interface between the first αβα domain of M-Hsp90 and N-Aha1, centred on the hydrophobic interaction between Ile 64, Leu 66 and Phe 100 from Aha1 and Leu 315, Ile 388 and Val 391 from Hsp90. Above this, the two proteins interact via a 'ladder' of ion pairs formed between Asp 53, Asp 101, Asp 68 and Glu 97 from Aha1, and lysines 387, 390, 394 and 398 from Hsp90. Side chains of Hsp90 residues are shown in white, and those of Aha1 in cyan.

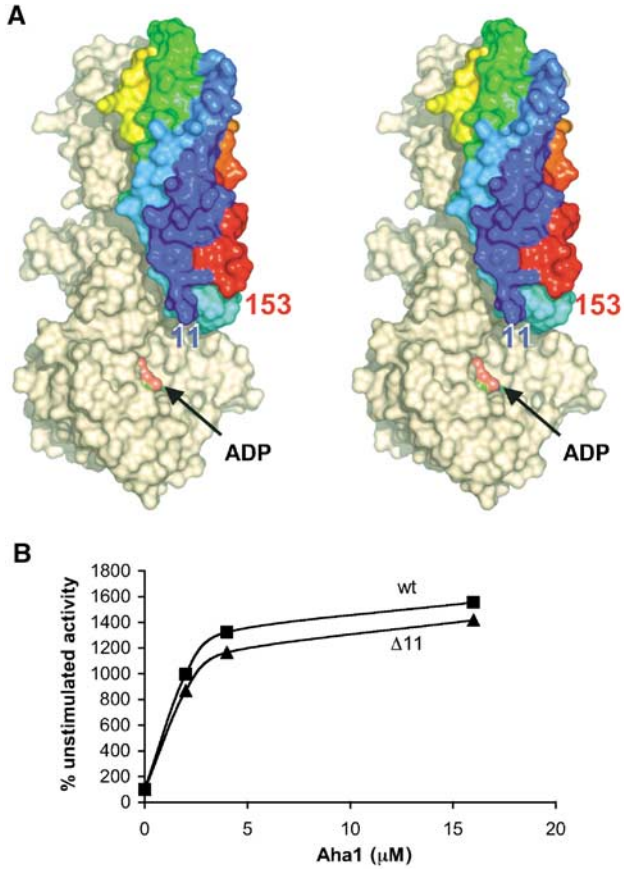

Figure 4 Aha1 proximity to the nucleotide-binding domain. (**A**) Docking of the crystal structure of the M-Hsp90–N-Aha1 complex onto the model for the combined N-terminal and middle segments of an Hsp90 monomer (Meyer *et al*, 2003) directs the C-terminus of the Aha1 N-terminal domain (rainbow coloured) towards the nucleotide-binding domain of Hsp90. The C-terminal domain of Aha1, which is not present in the smaller Hch1 homologue, could interact with the nucleotide-binding domain to further enhance ATP turnover. (**B**) Comparison of stimulation of yeast Hsp90 ATPase activity by wild type (wt) and Δ11-Aha1, in which the disordered N-terminal 11 residues have been deleted. Although it contains the NxNNWHW motif, which is highly conserved in Aha1 and Hch1 sequences, deletion of the N-terminal 11 residues produced only a very small decrease in the degree of activation elicited by Aha1, suggesting that it is not involved in the activation mechanism.

Consistent with its proposed biological role, those residues in Aha1 that are involved in binding Hsp90 are among the most conserved between different species (Figure 1), although Aha1 sequences themselves are far more diverged than those of Hsp90. However, one of the most highly conserved segments of sequence in Aha1 (and Hch1) occurs at the extreme N-terminus (5-NPNNWHW–11) and is disordered in the higher-resolution crystal form, and in all but one of the complexes in the lower-resolution crystals, where it is partly ordered by a nonspecific crystal lattice contact. Despite its lack of order, on the basis of the Aha1(1–153)–Hsp90(273–530) complex structure, this Trp/Asn-rich conserved N-terminal motif in Aha1 and Hch1 would approach the expected position of the N-terminal nucleotide-binding domain of Hsp90 in the intact protein complex (Figure 4A) and could therefore play a role in modulating the ATPase activity of the chaperone. To test this, we analysed the ability of Aha1 mutants with this N-terminal segment deleted, to assist Hsp90-dependent v-Src activation *in vivo* and/or to stimulate Hsp90 ATPase *in vitro*. Surprisingly, loss of this conserved motif did not impair the function of full-length Aha1 *in vivo* (data not shown), nor did it significantly alter the ability of Aha1 to stimulate Hsp90s ATPase activity *in vitro* (Figure 4B).

The lack of significant effect on Hsp90 ATPase activation when this highly conserved motif is deleted from Aha1, suggests that is involved in some other aspect of Aha1 function.

Conformational switching in the catalytic loop

While the N-terminal domain of Hsp90 provides all the interactions required for binding ATP, in isolation it has negligible ATPase activity (Prodromou *et al*, 2000) as it lacks a key catalytic residue required for orientating and polarising the γ-phosphate of ATP. Structural homology to other GHKL-family ATPases GyrB and MutL suggests that this function in Hsp90 is provided by Arg 380 in the 370–390 loop connecting the end of strand d and the beginning of helix 2 in the middle segment (Meyer *et al*, 2003) (Figure 5A). This is supported experimentally by complete loss of Hsp90 ATPase activity when Arg 380 is mutated (Meyer *et al*, 2003).

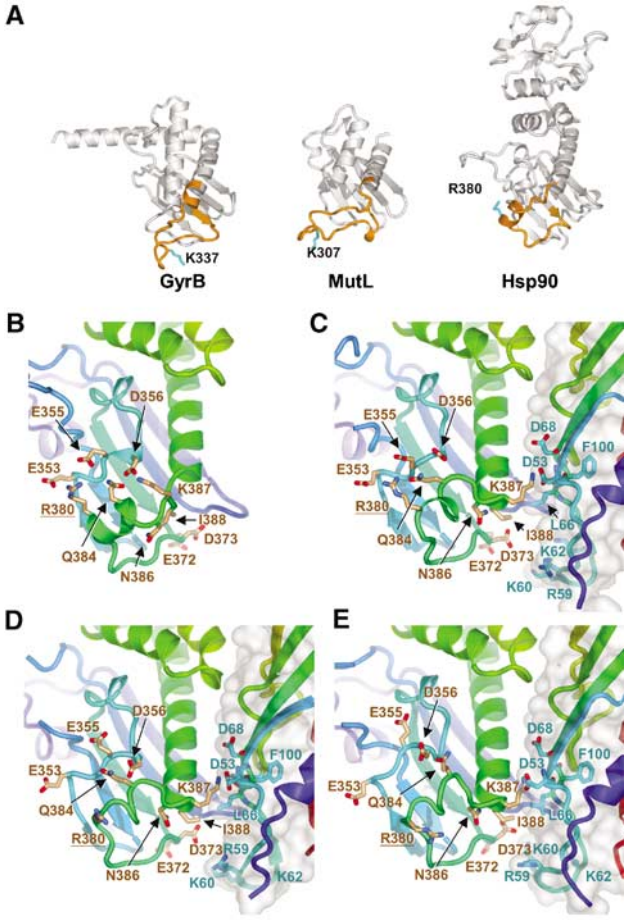

Figure 5 Conformational switching in the γ-phosphate-binding loop. (**A**) Comparison of the conformations of the γ-phosphate-binding loops (highlighted in gold) from the distantly related GHKL-family proteins GyrB, MutL and Hsp90. In the GyrB and MutL structures, where the N-terminal domain (not shown) contains a bound ATP analogue, the loops adopt an active conformation in which the catalytically essential basic residue (cyan) can contact the γ-phosphate. In uncomplexed Hsp90 in the absence of a nucleotide-bound N-terminal domain, the loop adopts a retracted structure with a short helix, in which the catalytic Arg 380 points back to the middle segment. (**B**) Detailed view of the retracted conformation of the catalytic loop (370–390) in Hsp90. Gln 384 and Lys 387, and the catalytically essential Arg 380 make ion-pair and polar interactions with a series of acidic residues (Glu 353, Glu 355 and Asp 356) on the overlying structure. (**C**) Detailed view of the catalytic loop of Hsp90 in the M-Hsp90–N-Aha1 complex. Binding of Aha1 causes the side chain of Lys 387 to move >15 Å, breaking its intramolecular ion-pair interaction with Asp 356 to hydrogen bond to the main-chain carbonyl of Leu 66 and ion pair with the side-chain carboxyl of Asp 53 of Aha1. Simultaneously, Ile 88 moves >8 Å to pack against the side chain of Leu 66 on Aha1. These movements add an extra turn to the beginning of the long helix following the catalytic loop in Hsp90, and destabilise the short helix (379–386), releasing Arg 380 from its retracted and inactive interaction with Glu 353 and Glu 355. (**D**, **E**) As (C), but from two other crystallographically independent copies of the M-Hsp90–N-Aha1 complex, showing the plasticity of the Hsp90 middle-segment catalytic loop.

Comparison of the structure of the middle segment of Hsp90 in free and Aha1-bound crystals suggests that ATPase activation by N-Aha1 and Hch1 involves a conformational switch in the catalytic loop (370–390) of Hsp90. In the uncomplexed structure of the Hsp90 middle segment, the chain emerging from the end of the central β-sheet at Glu 372 forms a short α-helix N-terminally capped by Ser 379 and ending with Asn 386. From here the chain connects via Lys 387 and Ile 388 to the N-terminus of a long α-helix starting at Met 389. In the short helix, the side chains of Leu 378 and Leu 383 pack back into the hydrophobic core, while the side chains of Arg 380, Gln 384 and Lys 387 are involved in polar interactions with Glu 353, Glu 355 and Asp 356 in an overlying region of the middle segment. In this conformation, the key catalytic residue Arg 380 is directed away from the expected position of the N-terminal nucleotide-binding domain and would be unable to interact with the γ-phosphate of bound ATP in the same way as the catalytic lysines in the equivalent region of MutL and GyrB (Figure 5A and B). In all of the five crystallographically independent views of the M-Hsp90–N-Aha1 complex available from the two crystal forms, the long α-helix becomes extended by one complete turn at the N-terminus, compared with the structure in the absence of Aha1 (Figure 5B–D). This additional turn of helix incorporates Lys 387 and Ile 388, whose side chains move by >15 and >8 Å, respectively, into the core interaction with Aha1, while the side chain of Asn 386 now provides the N-terminal cap to this extended α-helix. Recruitment of Ile 388, Lys 387 and Asn 386 into the long helix 'steals' residues from the short helix present in the free structure, substantially destabilising it and releasing Arg 380 from interaction with Glu 353 and Glu 355. In the higher-resolution crystal form of the M-Hsp90–N-Aha1 complex, residues 379–383 are disordered. However in the four copies of the complex in the second crystal form, ordered but subtly different structures are visible for this segment. The core interactions are similar in all cases, but reflecting its plasticity there are small variations in the conformation of the 370–390 loop, in the degree of interaction with Aha1, and in the extent to which Arg 380 is detached from its retracted conformation (with knock-on effects on the conformation of the overlying loop containing the acidic residues Glu 353, Glu 355 and Asp 356).

That the conformational change observed in the 370–390 loop releases Arg 380 to access the ATP binding site in the N-terminal domain of Hsp90 (Meyer *et al*, 2003) suggests a role in the mechanism of ATPase activation common to both Aha1 and Hch1. We therefore analysed the effect on ATPase activation of a series of N-Aha1 mutations in polar residues involved in interactions with the 370–390 loop in Hsp90, by mutation of Lys 387 in Hsp90 itself, which undergoes the largest movement on Aha1 binding, and by mutation of Asp 53 in N-Aha1, which interacts with Lys 387. As the conformational change in the 370–390 loop of Hsp90 appears to be dependent on Aha1 binding, the processes of binding and activation cannot be truly separated, and any mutation that diminishes activation will inevitably decrease the affinity of the interaction. To help deconvolute these coupled effects, the effectiveness of the Aha1 mutants in activating Hsp90 ATPase was determined at a range of Aha1 concentrations ranging from equimolar with Hsp90 to 32-fold molar excess. Effects on affinity can then be seen as changes in the concentration at which Aha1 mutants achieve half-maximal effect (EC_{50}), while effects on activation itself are shown by the maximal effect at saturation, at which point all the Hsp90 is fully bound by the N-Aha1 or mutant protein. Thus, if the decreased activation observed for a mutant were purely due to decreased affinity, the curve will shift to the right but tend to the same maximal activation at saturation, whereas if wild-

type activation is not attained at full saturation, the mutation is directly affecting the activation mechanism.

Arg 59, and Lys 60 and 62 are part of a basic motif 59-RKGK-62, which occurs at the flexible tip of the loop connecting strands a′ and b in Aha1, and is totally conserved in the Aha1/Hch1 family. In all copies of the complex with Hsp90, the side chains of these residues are directed towards Hsp90 and form ion-pair interactions with Glu 372 and Asp 373 at the beginning of the catalytic loop, which would serve to stabilise the loop in its active conformation. Consistent with this role, mutation of any of these residues to alanine caused a significant decrease in the ability of Aha1 to stimulate ATPase activity at saturation, most marked for Lys 60 which comes closest to Glu 372 and Asp 373 in the complex with Hsp90, but with only small increases in the corresponding EC_{50} (Figure 6A). The K_d for the interaction of K60A N-Aha1 with Hsp90 determined by ITC was 5.7 μM compared to 1.75 μM for the wild-type N-Aha1 (data not shown), confirming that the concentrations used were truly saturating, and the effects observed can be attributed to defects in the mechanism of activation, and not to the small decrease in affinity.

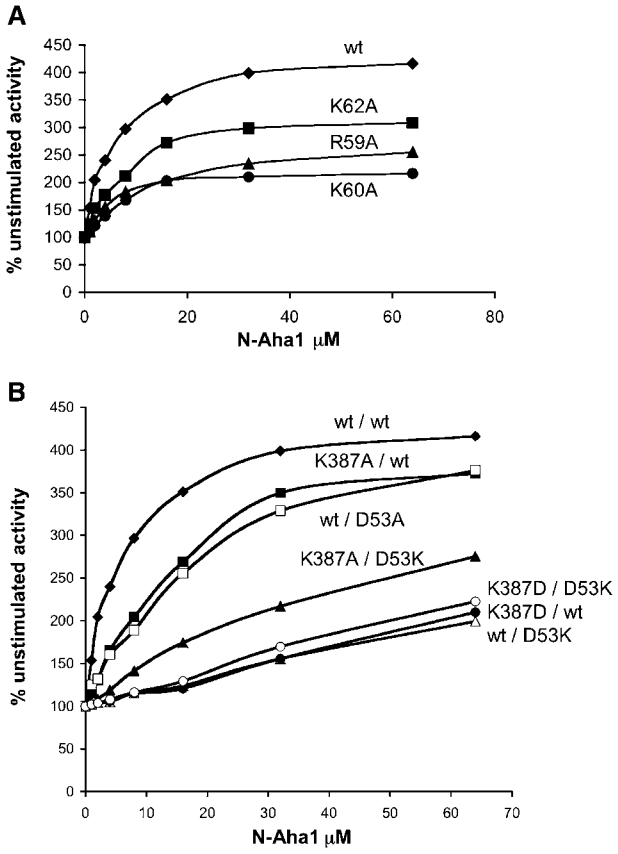

Figure 6 Functional analysis of Hsp90–Aha1 interacting residues. (**A**) The basic RKGK motif in Aha1 forms ion pairs with acidic side chains in the catalytic loop that will stabilise the active conformation. Mutation of all these residues to alanine produces a substantial decrease in ATPase activation as judged by the maximal activation achieved at saturation, but with little decrease in affinity. (**B**) Asp 53 in Aha1 and Lys 387 in Hsp90 form part of the core interaction between the two proteins following a binding-induced conformational change in the 370–390 loop of Hsp90. Mutation of either of these residues to alanine, which permits the conformational change, causes a decrease in affinity but only a small decrease in ATPase activation. Charge-reversal mutations at either residue prevent adoption of the binding-induced conformation and substantially decreases activation and affinity.

Residues 386–388 in Hsp90 undergo a large conformational change upon binding of N-Aha1, with the side chain of Lys 387 in particular moving >15 Å to hydrogen bond to the backbone carbonyl of Leu 66 and the carboxyl side chain of Asp 53 from N-Aha1 (see above). As the residues in this segment form a substantial part of the core interaction with Aha1, mutations that affect their ability to undergo this conformational change would be expected to have significant effects on activation and binding. Mutation of Lys 387 to alanine, which would weaken but not prevent the Aha1-induced conformation, caused a small decrease in affinity for N-Aha1 ($K_d = 8.5$ μM by ITC) compared to wild type, but the K387A Hsp90 could be activated to ∼90% wild-type levels at saturation (Figure 6B). The complementary D53A mutation in N-Aha1, which would also permit the conformational change, behaved in a similar fashion when combined with wild-type Hsp90. In contrast, the Hsp90 K387D charge-reversal mutation, which would positively obstruct the conformational change, produced a substantial loss of activation accompanied by a large decrease in affinity ($K_d = 37$ μM by ITC). The complementary D53K mutation in N-Aha1 produced a similar loss of activation with wild-type or mutant Hsp90s.

Discussion

Co-chaperone interactions

Hsp90 is the central component of an ordered set of dynamic and interchanging multiprotein complexes with co-chaperones, which facilitates the activation of Hsp90-dependent client proteins (reviewed in Pearl and Prodromou, 2002; Pratt and Toft, 2003). Thus, in addition to binding the client proteins themselves, Hsp90 must provide binding sites for the various co-chaperones, some of which additionally interact with the client protein and with each other. Hitherto, the only co-chaperone interaction site mapped onto Hsp90 at the molecular level (Scheufler *et al*, 2000) was the C-terminal MEEVD peptide that binds to tetratricopeptide-repeat (TPR) domains in co-chaperones such as the immunophilins FKBP52 and Cyp40 (Owens-Grillo *et al*, 1996a, b; Ratajczak and Carrello, 1996), Cns1 (Dolinski *et al*, 1998; Marsh *et al*, 1998), Hop/Sti1 (Chen *et al*, 1998) and the protein phosphatase PP5/Ppt1 (Silverstein *et al*, 1997). The structure of the Hsp90–Aha1 core complex is significantly different from these and provides the first observation of a protein–protein interaction between Hsp90 and one of its co-chaperones. Primary interaction of Aha1 with the middle segment of Hsp90 confirms previous biochemical data (Meyer *et al*, 2003), and is fully consistent with the observation that Aha1 can coexist in Hsp90-based complexes with TPR-domain co-chaperones (Panaretou *et al*, 2002), which are mutually exclusive among themselves for binding to their C-terminal binding site (Owens-Grillo *et al*, 1995, 1996a).

Activation mechanism

The Aha1(1–153) domain within the core complex is equivalent to the entire structure of the homologous Hch1 ATPase activating co-chaperone, and provides ≈40% of the affinity for Hsp90, and ∼1/3 of the ATPase activation (Panaretou *et al*, 2002) of full-length Aha1. While this part of Aha1 is not

sufficient for the maximal activation elicited by the full-length protein, it is absolutely necessary for that activation, as the C-terminal part of Aha1, which is not present in Hch1, has no ability to activate Hsp90 in isolation. Thus, the primary mechanism of Hsp90 ATPase activation common to the Aha1 and Hch1 co-chaperones lies within the structure presented here.

The available biochemical and genetic evidence points at the loop from residues 370–390 connecting the end of strand d and the beginning of helix 2 in the middle segment of Hsp90, as the point at which Aha1/Hch1 exerts its influence. Direct involvement of this loop in catalysis is suggested by structural homology to other GHKL-family ATPases GyrB and MutL, where the equivalent segments provide the key catalytic contact(s) for the γ-phosphate of ATP bound in the N-terminal domain. This is supported experimentally by complete loss of Hsp90 ATPase activity when Arg 380 and, to a lesser extent, Gln 384 in this loop are mutated (Meyer *et al*, 2003). Interaction of this loop with Aha1/Hch1 is suggested by the ability of Hch1 overexpression to suppress the *in vivo* temperature sensitivity of the yeast Hsp90 mutant E381K, which maps in this loop (Nathan *et al*, 1999), and the substantially reduced sensitivity of the E381K mutant to ATPase activation by Aha1 *in vitro* (Panaretou *et al*, 2002). Together with the structure of the M-Hsp90–N-Aha1 complex presented here, these data provide compelling circumstantial evidence for a mechanism in which N-Aha1 or Hch1 facilitate and/or stabilise a conformational switch in the catalytic 370–390 loop in the middle segment of Hsp90, which enhances its ATPase activity.

In the isolated Hsp90 middle segment, the catalytic loop shows a substantial degree of conformational plasticity with three different ordered conformations observed in separate molecules in two crystal forms (Meyer *et al*, 2003). In the most ordered of these conformations, the critical catalytic residue Arg 380 is directed away from the N-terminal domain and tucked back into the body of the middle segment in a catalytically inactive conformation (Figure 5A and B). Some insight into the 'active' conformation required for this loop can be gained by comparison with the topologically equivalent loops in the distantly related MutL and GyrB proteins, for both of which there are structures containing the N-terminal and following domains, in complex with the nonhydrolysable ATP analogue AMPPNP (Wigley *et al*, 1991; Ban *et al*, 1999). In both cases the loop, equivalent to the catalytic loop in Hsp90, forms an ordered hairpin structure with the side chain of a lysine residue at the tip (Lys 307 in MutL; Lys 335 in GyrB) pointing down towards the γ-phosphate of AMPPNP bound in the N-terminal domain (Figure 5A). The catalytic loop in Hsp90 is four residues shorter, but would be perfectly capable of forming a similar hairpin structure to the MutL and GyrB equivalents, with the side chain of Arg 380 directed towards the γ-phosphate of a bound ATP. However, in the absence of such contacts, and unlike the equivalent in MutL (Ban and Yang, 1998), the Hsp90 loop has a well-ordered alternative and catalytically inactive conformation in which Arg 380 binds back into the middle segment. Redirection of Arg 380 towards an ATP bound in the N-terminal domain would require melting of the local helical secondary structure and disruption of all of these side-chain interactions, presenting an energetic barrier to that conformational change. As positioning and neutralisation of the γ-phosphate is critical for ATP hydrolysis, a conformational switch in the 370–390 loop from the retracted helical conformation to an extended hairpin loop is likely to be a rate-limiting event.

In the M-Hsp90–N-Aha1 complex presented here, binding of N-Aha1 is accompanied by conformational changes in the 370–390 loop that release Arg 380 from its retracted inactivating conformation. This strongly suggests that the mechanism of activation by N-Aha1/Hch1 Hsp90 proceeds via induced remodelling of the γ-phosphate-binding loop. Consistent with this, disruptive mutations of residues involved in the core interaction between the remodelled 370–390 Hsp90 loop and N-Aha1 substantially impaired ATPase activation. However, mutations in the RKGK motif that interacts with acidic groups at the start of the 370–390 loop produced an almost pure loss of activation, with only a small decrease of affinity. Although binding and remodelling are inextricably linked, decreased activation and decreased affinity are not simply correlated. Thus, N-Aha1-K60A and Hsp90 bind to each other with higher affinity than N-Aha1 and Hsp90-K387A (K_d 5.7 and 8.5 μM, respectively, by ITC), but with only ∼40% of the ATPase activity at saturation (Figure 6A and B).

Hsp90 regulation

While Hsp90 in isolation possesses a weak inherent ATPase activity *in vitro*, it is becoming clear that this activity *in vivo* will be tightly regulated by interactions with the various Hsp90-associated co-chaperones, which participate in the dynamic series of complexes that accompanies the ATPase-coupled chaperone cycle. Hop/Sti1 and Cdc37/p50^{cdc37} inhibit ATP turnover in the early phase of the cycle in which client proteins are loaded onto Hsp90 (Prodromou *et al*, 1999; Siligardi *et al*, 2002). The mechanism of this inhibition is unclear, but at least for Hop/Sti1 may involve stabilisation of the dimeric Hsp90 molecular clamp in an open conformation in which the N-terminal nucleotide-binding domains cannot associate (Prodromou *et al*, 2000; Richter *et al*, 2003). The 'late' co-chaperone p23/Sba1, which only associates with Hsp90 in the ATP-bound and N-terminally dimerised form (Chadli *et al*, 2000; Prodromou *et al*, 2000; Sullivan *et al*, 2002), slows down the cycle by stabilising the closed conformation of the clamp, but as it binds after ATP, it cannot completely inhibit the ATPase activity (Panaretou *et al*, 2002). The mechanism by which p23/Sba1 stabilises the closed conformation of ATP-bound Hsp90 has not yet been determined, but most likely involves the formation of a structural bridge between associated N-terminal domains in the dimer.

An ability to activate the Hsp90 ATPase has now been found in two co-chaperones. The TPR-domain cyclophilin Cpr6/Cyp40 stimulates the ATPase activity of yeast Hsp90 up to two-fold, a property that does not require its peptidyl prolyl isomerase domain (Panaretou *et al*, 2002). A far more substantial degree of Hsp90 ATPase activation is displayed by the recently described Aha1 (more than 50-fold for hHsp90β) and, to a lesser extent, its smaller homologue Hch1 (Panaretou *et al*, 2002; Lotz *et al*, 2003). Activation by Cpr6 and Aha1 is synergistic, suggesting that they operate by complementary mechanisms. The data presented here show that a substantial part of the activation mechanism for the Aha1/Hch1 co-chaperones involves facilitating a conformational switch in the γ-phosphate-binding loop of the Hsp90 middle segment, from a retracted and inactive state, into an

extended conformation in which the catalytic Arg 380 can access the nucleotide bound to the N-terminal domain.

Materials and methods

Protein expression and purification

Constructs of the middle region (273–530) of yeast Hsp90 (M-Hsp90), and of the N-terminal Hch1-homologous region (1–153) of yeast Aha1 (N-Aha1), both with N-terminal His_6-tag, were inserted into pRSETA and expressed in *Escherichia coli* BL21(DE3) pLysS as previously described (Panaretou *et al*, 2002; Meyer *et al*, 2003). In both cases expressed proteins were purified by metal affinity chromatography on Talon resin, ion exchange on Q-sepharose, and size-exclusion chromatography on a Superdex 75 PG column equilibrated in 20 mM Tris pH 7.5, 150 mM NaCl, 1 mM EDTA and 0.5 mM DTT (buffer A). Fractions containing pure proteins were dialysed against buffer A and finally concentrated using 5 K Vivaspin concentrators.

Crystallisation of the M-Hsp90/N-Aha1 complex

High diffraction quality crystals (crystal 1) grew from a mixture of M-Hsp90 and N-Aha1 at a final concentration of 110 and 165 μM, respectively, in a solution containing 90 mM ammonium sulphate, 13.5%. (w/v) polyethylene glycol 8000 and 45 mM sodium cacodylate (pH 6.5) in under-oil microbatch experiments at 19°C.

A second crystal form (crystal 2) was obtained from a mixture of M-Hsp90 and N-Aha1 at a final concentration of 130 and 195 μM, respectively, in a solution containing 560 mM tri-sodium citrate dihydrate (pH 6.5) in under-oil microbatch experiments at 19°C.

Crystallographic data collection, phasing and refinement

Crystals were transferred through crystallisation buffers with progressively higher glycerol concentration up to 20% v/v and then flash cooled in liquid nitrogen. Crystals of the first form (crystal 1) had space group $P2_1$ with unit cell dimensions $a = 58.9$ Å, $b = 37.9$ Å, $c = 111.3$ Å and $\beta = 97.7°$. A data set was collected on beamline ID14-1 at ESRF Grenoble. Image processing and data reduction were carried out using MOSFLM (Leslie, 1995), and scaled and merged using programs of the CCP4 suite (CCP4, 1994). A molecular replacement solution was found with AmoRe (Navaza, 1994) using the structure of the central region of Hsp90 (PDB code 1HK7) as a search model. The correct solution showed a correlation coefficient of 33.9 and an *R*-factor of 48.4 with one molecule of the Hsp90 middle segment per asymmetric unit. This solution gave a map of good quality in which the N-Aha1 structure was clearly visible. The majority of the Aha1 moiety was built at this stage using TURBO (Roussel and Cambillau, 1991), and the resulting structure was refined using CNS (Brunger *et al*, 1998) together with manual correction with TURBO and O (Jones *et al*, 1991).

Crystals of the second form have the space group $P2_1$ with unit cell dimensions $a = 58.4$ Å, $b = 207.9$ Å, $c = 84.5$ Å and $\beta = 98.4°$. A data set was collected on beamline ID14-1 at ESRF Grenoble, and processed as for crystal form 1. The structure was solved by molecular replacement using AmoRe with the refined structure from crystal 1 as the search model. The correct solution showed a correlation coefficient of 62.3 and an *R*-factor of 39.5 with four M-Hsp90/N-Aha1 complexes in the asymmetric unit, and was subsequently refined using the procedure described for crystal 1.

Statistics for the data collections and refinements are given in Table I. Coordinates have been deposited in the Protein Databank with accession codes 1USU and 1USV. Molecular graphics were generated with PyMol (DeLano Scientific www.pymol.org).

Table I Crystallographic statistics

	Form 1	Form 2
Data set (crystal)		
Wavelength (Å)	0.934	0.934
Beamline	ID14-EH2	ID14-EH1
Resolution (Å)	2.15	2.7
Observations	26832	53437
Completeness (%)	99.1 (99.0)	98.0 (94.5)
Multiplicity	3.6	3.0
R_{merge} (%)	8.9 (30.2)	10.4 (33.8)
$I/\text{sig}I$	4.0 (2.3)	4.3 (2.2)
Refinement		
Resolution range (Å)	100–2.15	100–2.7
Number of reflections	26818	53402
Number of protein atoms	3070	12731
Number of solvent atoms	234	58
R_{cryst}/R_{free} (%)	21.4/26.8	22.9/29.9
RMSD bond lengths (Å)	0.016	0.008
RMS bond angles (°)	1.74	1.37

Mutagenesis and ATPase activation assays

N-Aha1 mutants D53A (GAT to GCT), D53K (GAT to AAG), R59A (CGT to GCT), K60A (AAG to GCG) and K62A (AAG to GCG), and Hsp90 mutants K387A (AAG to GCG) and K387D (AAG to GAT) were generated using the Stratagene Quick Change site-directed mutagenesis kit, according to the manufacturer's instructions. Mutant proteins were expressed in *E. coli* and purified as the wild type (see above).

ATPase activity of purified Hsp90 was measured using an enzyme-linked spectrophotometric assay as previously described (Panaretou *et al*, 1998; Panaretou *et al*, 2002). Activation by wild type and Δ11-Aha1 was determined by additions of 2, 4 and 16 μM of Aha1 to 2 μM Hsp90 at 37°C. For N-Aha1 assays, 0.5, 1, 2, 4, 8, 16, 32 and 64 μM N-Aha1, D53A, D53K, R59A, K60A or K62A mutant was added to 2 μM wild-type, K387A or K387D Hsp90 at 37°C.

Isothermal titration calorimetry

Heats of interaction between Hsp90 and N-Aha1 constructs were measured on an MSC system (Microcal Inc.). Fifteen aliquots of 20 μl Aha1, N-Aha1 or mutant were injected into 1.458 ml of 34.2 μM full-length Hsp90, mutant Hsp90 or Hsp90(273–560) at 30°C in 40 mM Tris (pH 8.0) containing 1 mM EDTA and 5 mM NaCl. The injected Aha1 proteins were either at 324 or 267 μM. After subtracting the heats of dilution, determined in a separate experiment by diluting protein in buffer, the resulting data were fitted using a nonlinear least-squares curve-fitting algorithm (Microcal Origin) with three floating variables: stoichiometry, binding constant and change of enthalpy of interaction.

Acknowledgements

This work was supported by the Wellcome Trust (LHP, BP) and Medical Research Council (LHP). BH gratefully acknowledges the support of the KC Wong Education Foundation and China Scholarship Council. We are very grateful to ESRF Grenoble for access to synchrotron radiation, to Cancer Research UK for infra-structural support for Structural Biology at The Institute of Cancer Research, and to for technical assistance. BH is a visiting Doctoral Scholar from the College of Life Science, Zhejiang University, China.

References

Ban C, Junop M, Yang W (1999) Transformation of MutL by ATP binding and hydrolysis: a switch in DNA mismatch repair. *Cell* **97:** 85–97

Ban C, Yang W (1998) Crystal structure and ATPase activity of MutL: implications for DNA repair and mutagenesis. *Cell* **95:** 541–552

Beamer LJ, Carroll SF, Eisenberg D (1997) Crystal structure of human BPI and two bound phospholipids at 2.4 angstrom resolution. *Science* **276:** 1861–1864

Brunger AT, Adams PD, Clore GM, DeLano WL, Gros P, Grosse-Kunstleve RW, Jiang JS, Kuszewski J, Nilges M, Pannu NS, Read RJ, Rice LM, Simonson T, Warren GL (1998) Crystallography & NMR system: a new software suite for macromolecular structure determination. *Acta Crystallogr* **D54:** 905–921

CCP4 (1994) Programs for protein crystallography. *Acta Crystallogr* **D50:** 760–763

Chadli A, Bouhouche I, Sullivan W, Stensgard B, McMahon N, Catelli MG, Toft DO (2000) Dimerization and N-terminal domain proximity underlie the function of the molecular chaperone heat shock protein 90. *Proc Natl Acad Sci USA* **97:** 12524–12529

Chen S, Smith DF (1998) Hop as an adaptor in the heat shock protein 70 (Hsp70) and Hsp90 chaperone machinery. *J Biol Chem* **273:** 35194–35200

Chen SY, Prapapanich V, Rimerman RA, Honore B, Smith DF (1996) Interactions of p60, a mediator of progesterone-receptor assembly, with heat-shock proteins hsp90 and hsp70. *Mol Endocrinol* **10:** 682–693

Chen SY, Sullivan WP, Toft DO, Smith DF (1998) Differential interactions of p23 and the TPR-containing proteins Hop, Cyp40, FKBP52 and FKBP51 with Hsp90 mutants. *Cell Stress Chaper* **3:** 118–129

Dolinski KJ, Cardenas ME, Heitman J (1998) CNS1 encodes an essential p60/Sti1 homolog in *Saccharomyces cerevisiae* that suppresses cyclophilin 40 mutations and interacts with Hsp90. *Mol Cell Biol* **18:** 7344–7352

Grammatikakis N, Lin J-H, Grammatikakis A, Tsichlis PN, Cochran BH (1999) p50cdc37 acting in concert with Hsp90 is required for Raf-1 function. *Mol Cell Biol* **19:** 1661–1672

Jones TA, Zou J-Y, Cowan SW, Kjeldgaard M (1991) Improved methods for building protein models in electron density maps and the location of errors in these models. *Acta Crystallogr* **A47:** 110–119

Leslie AGW (1995) *MOSFLM Users Guide*. Cambridge, UK: MRC Laboratory of Molecular Biology

Lotz GP, Lin H, Harst A, Obermann WMJ (2003) Aha1 binds to the middle domain of Hsp90, contributes to client protein activation, and stimulates the ATPase activity of the molecular chaperone. *J Biol Chem* **278:** 17228–17235

Marsh JA, Kalton HM, Gaber RF (1998) Cns1 is an essential protein associated with the Hsp90 chaperone complex in *Saccharomyces cerevisiae* that can restore cyclophilin 40-dependent functions in *cpr7delta* cells. *Mol Cell Biol* **18:** 7353–7359

Meyer P, Prodromou C, Hu B, Vaughan C, Roe SM, Panaretou B, Piper PW, Pearl LH (2003) Structural and functional analysis of the middle segment of Hsp90: implications for ATP hydrolysis and client-protein and co-chaperone interactions. *Mol Cell* **11:** 647–658

Nathan DF, Vos MH, Lindquist S (1999) Identification of SSF1, CNS1, and HCH1 as multicopy suppressors of a *Saccharomyces cerevisiae* Hsp90 loss-of-function mutation. *Proc Natl Acad Sci USA* **96:** 1409–1414

Navaza J (1994) AMoRE—an automated package for molecular replacement. *Acta Crystallogr* **D50:** 157–163

Obermann WMJ, Sondermann H, Russo AA, Pavletich NP, Hartl FU (1998) *In vivo* function of Hsp90 is dependent on ATP binding and ATP hydrolysis. *J Cell Biol* **143:** 901–910

Owens-Grillo JK, Czar MJ, Hutchinson KA, Hoffman K, Perdew GH, Pratt WB (1996a) A model of protein targetting mediated by immunophilins and other proteins that bind to hsp90 via tetratricopeptide repeat domains. *J Biol Chem* **271:** 13468–13475

Owens-Grillo JK, Hoffman K, Hutchinson KA, Yem AW, Deibel MRJ, Handschumacher RE, Pratt WB (1995) The cyclosporin A-binding immunophilin Cyp-40 and the FK506-binding immunophilin hsp56 bind to a common site on hsp90 and exist in independent cytosolic heterocomplexes with the untransformed glucocorticoid receptor. *J Biol Chem* **270:** 20479–20484

Owens-Grillo JK, Stancato LF, Hoffmann K, Pratt WB, Krishna P (1996b) Binding of immunophilins to the 90 kDa heat shock protein (hsp90) via a tetratricopeptide repeat domain is a conserved protein interaction in plants. *Biochemistry* **35:** 15249–15255

Panaretou B, Prodromou C, Roe SM, O'Brien R, Ladbury JE, Piper PW, Pearl LH (1998) ATP binding and hydrolysis are essential to the function of the Hsp90 molecular chaperone *in vivo*. *EMBO J* **17:** 4829–4836

Panaretou B, Siligardi G, Meyer P, Maloney A, Sullivan JK, Singh S, Millson SH, Clarke PA, Naaby-Hansen S, Stein R, Cramer R, Mollapour M, Workman P, Piper PW, Pearl LH, Prodromou C (2002) Activation of the ATPase activity of Hsp90 by the stress-regulated co-chaperone Aha1. *Mol Cell* **10:** 1307–1318

Pearl FMG, Lee D, Bray JE, Sillitoe I, Todd AE, Harrison AP, Thornton JM, Orengo CA (2000) Assigning genomic sequences to CATH. *Nucleic Acids Res* **28:** 277–282

Pearl LH, Prodromou C (2002) Structure, function and mechanism of the Hsp90 molecular chaperone. *Adv Prot Chem* **59:** 157–185

Pratt WB, Toft DO (2003) Regulation of signaling protein function and trafficking by the hsp90/hsp70-based chaperone machinery. *Exp Biol Med* **228:** 111–133

Prodromou C, Panaretou B, Chohan S, Siligardi G, O'Brien R, Ladbury JE, Roe SM, Piper PW, Pearl LH (2000) The ATPase cycle of Hsp90 drives a molecular 'clamp' via transient dimerization of the N-terminal domains. *EMBO J* **19:** 4383–4392

Prodromou C, Roe SM, O'Brien R, Ladbury JE, Piper PW, Pearl LH (1997) Identification and structural characterization of the ATP/ADP-binding site in the Hsp90 molecular chaperone. *Cell* **90:** 65–75

Prodromou C, Siligardi G, O'Brien R, Woolfson DN, Regan L, Panaretou B, Ladbury JE, Piper PW, Pearl LH (1999) Regulation of Hsp90 ATPase activity by tetratricopeptide repeat (TPR)-domain co-chaperones. *EMBO J* **18:** 754–762

Ratajczak T, Carrello A (1996) Cyclophilin-40 (Cyp-40), mapping of its Hsp90 binding domain and evidence that FKBP52 competes with Cyp-40 for Hsp90 binding. *J Biol Chem* **271:** 2961–2965

Richter K, Muschler P, Hainzl O, Reinstein J, Buchner J (2003) Sti1 is a non-competitive inhibitor of the Hsp90 ATPase. *J Biol Chem* **278:** 10328–10333

Roussel A, Cambillau C (1991) TURBO. In *Silicon Graphics Geometry Partners Directory*, Vol. **81**, pp 77–78. Mountain View, CA: Silicon Graphics Inc

Sato S, Fujita N, Tsuruo T (2000) Modulation of akt kinase activity by binding to hsp90. *Proc Natl Acad Sci USA* **97:** 10832–10837

Scheufler C, Brinker A, Bourenkov G, Pegoraro S, Moroder L, Bartunik H, Hartl FU, Moarefi I (2000) Structure of TPR domain-peptide complexes: critical elements in the assembly of the Hsp70-Hsp90 multichaperone machine. *Cell* **101:** 199–210

Siligardi G, Panaretou B, Meyer P, Singh S, Woolfson DN, Piper PW, Pearl LH, Prodromou C (2002) Regulation of Hsp90 ATPase activity by the co-chaperone Cdc37p/p50^{cdc37}. *J Biol Chem* **277:** 20151–20159

Silverstein AM, Galigniana MD, Chen M-S, Owens-Grillo J, Chinkers M, Pratt WB (1997) Protein phosphatase 5 is a major component of glucocorticoid receptor-hsp90 complexes with properties of an FK506-binding immunophilin. *J Biol Chem* **272:** 16224–16230

Sullivan WP, Owen BAL, Toft DO (2002) The influence of ATP and p23 on the conformation of hsp90. *J Biol Chem* **277:** 45942–45948

Wigley DB, Davies GJ, Dodson EJ, Maxwell A, Dodson G (1991) Crystal structure of an N-terminal fragment of the DNA gyrase B protein. *Nature* **351:** 624–629

Young JC, Hartl FU (2000) Polypeptide release by Hsp90 involves ATP hydrolysis and is enhanced by the co-chaperone p23. *EMBO J* **19:** 5930–5940

